Distortional Buckling of Cold-formed Steel Z-section Columns

P. Charnvarnichborikarn

Dimos Polyzois

Eleventh International Specialty Conference on Cold-Formed Steel Structures
St. Louis, Missouri, U.S.A., October 20-21, 1992

DISTORTIONAL BUCKLING OF COLD-FORMED STEEL Z-SECTION COLUMNS

P. Charnvarnichborikarn[1], and **D. Polyzois**[2], A.M. ASCE

ABSTRACT

Current North American guidelines for the design of cold-formed steel members consider the web of cold-formed steel sections under direct compression to be a fully stiffened element. This, however, may not be true if the flanges cannot provide sufficient restraint to the web. In this case, instability of the web element may cause distortional failure of the flange-edge stiffener component which may limit the load-carrying capacity of these sections with very little post-buckling strength being realized.

In the present paper, the effect of web buckling on the load-carrying capacity of Z-sections with partially stiffened flanges is examined. The current design criteria for cold-formed steel sections with edge stiffeners located perpendicular to the flanges are reviewed and evaluated through comparison with experimental data obtained in a test program involving 85 Z-sections loaded in direct compression with pin-ended condition. The Z-sections varied in length from 18 in. (459 mm) to 48 in. (1219 mm). The important parametric variations in these tests were the width-to-thickness ratio of the flanges, and the width of the edge stiffeners. Based on the results from this study, a procedure for predicting the load-carrying capacity of cold-formed steel Z-sections subject to local buckling of the web under direct compression was developed.

Key Words: Cold-Formed, steel, distortional buckling, edge stiffeners, Z-sections

INTRODUCTION

Cold-formed steel members, such as Z-sections, provide substantial savings due to their high strength-to-weight ratio. The cross sectional configuration of these sections, however, gives rise to behavioral phenomena, such as local and distortional buckling, which could effect the overall load-carrying capacity of these members. Edge stiffeners are added to the flanges to enhance the post-buckling strength of such sections. Local and distortional buckling are functions of the rigidity of the edge stiffeners. If the rigidity of the edge stiffeners is adequate, local buckling of the individual plate elements will take place, as shown in Figure 1a. In this case, the post-buckling capacity of the elements can be developed. On the other hand, if the rigidity of the edge stiffeners is inadequate, distortional buckling of the flange-edge stiffener components will take place, as shown in Figure 1b. The post-buckling capacity of the elements, in this case, may not be developed and the overall capacity of the member may be drastically reduced.

In the current North American design specifications for the design of cold-formed steel members, the concept of partially stiffened flanges is used. These specifications recognize the fact that an edge stiffener may not provide adequate rotational restraint to a compression flange and a buckling coefficient, which ranges from 0.43 for unstiffened flanges, to 4.0 for fully stiffened flanges is used. It is not clear, however, what the buckling coefficient of a web element should be. The practice has been to consider the web as a fully stiffened element. A buckling coefficient of 4.0 is used if the web is under direct compression. This, however, may not be true if the flanges of the sections cannot provide sufficient restraint to the web. A

[1]Grad. Student., Dept. of Civ. Eng., Univ. of Manitoba, Winnipeg, R3T 2N2, Canada.

[2]Assoc. Prof., Dept. of Civ. Eng., Univ. of Manitoba, Winnipeg, R3T 2N2, Canada.

premature failure of the compression flanges, such as distortional buckling, will cause buckling of the web at a stress well below the local buckling stress. Also if the web element becomes unstable first, distortional failure of the flange-edge stiffener component could take place. These phenomena will limit the load-carrying capacity of the cold-formed sections with very little post-buckling strength being realized.

In order to study the interaction between a locally destabilized web element and distortional buckling of flange-edge stiffener components, a research program involving both experimental and analytical work was carried out. The research program included columns, beams, and beam-columns. The present paper, however, deals only with the results of 85 Z-sections tested under direct uniform compression. Of these 45 specimens were 18 in. (457 mm) long (Rosner et al, 1989), 20 specimens were 24 in. (610 mm) long (Le et al, 1990), and 20 specimens were 48 in. (1219 mm) long (Charnvarnichborikarn and Polyzois, 1990). A simplified theoretical model was also developed for determining the load-carrying capacity of these Z-sections. The North American design guidelines, namely the American Specification (AISI, 1989) and Canadian Standard (CSA, 1989), for cold-formed Z-sections were evaluated through comparison with this experimental data.

EXPERIMENTAL INVESTIGATION

The test specimens were cold-formed by a commercial manufacturer using the press-brake operation from cold-rolled high-strength low alloy sheets (ASTM A607-90a Standard, 1991). A complete list of the parameters used in this experimental investigation, along with the number of specimens tested in each category, are given in Table 1. In this table, column (8) shows a group of specimens with unstiffened flanges. In these specimens there was no curved portion of edge stiffeners. Column (9) shows a group of specimens where the edge stiffeners had only a curved portion and no flat width. Also, the 18 in. (457 mm) specimens were uncoated, while the 24 and 48 in. (610 and 1219 mm) specimens were coated with a primer. To measure the base metal thickness of these specimens, the primer was removed by Polystrippa, a chemical solution. The actual cross sectional dimensions of the specimens tested are given in Tables 2 to 4. Three terms are used to identify the specimens. The first two terms are the nominal flat width of the flange and the edge stiffener, respectively, while the last term is the number of the specimen tested in that category.

All specimens were tested in a 60 kips (267 kN) capacity Riehle testing machine. The test set-up for a typical specimen is shown in Figure 2. The load was applied through hemispherical loading cylinders bearing against a rigid steel plate placed at the ends of the specimens, as shown in Figure 3, to ensure uniform compressive load. Also shown in this figure, 0.5 in. (13 mm) thick adjustable bars were bolted to the support plates to provide lateral support to the ends of the specimen and to prevent the specimen from slipping off the support plates after local buckling. A small circular "dent" was made on the reverse side of the support plates to coincide with the centroid of the Z-section. The hemispherical loading cylinders would rest in the dent of the plates and be restrained from moving during testing. The vertical alignment of the specimens was checked with a carpenter's level.

To ensure that the buckling behaviour of the specimen was observed, a rate of loading equal to 0.5 kips/min (0.23 kN/min) was used. The instrumentation included three Linear Variable Differential Transducers (LVDT's) and one load cell. The LVDT's were used to measure the longitudinal deformation and the mid-height displacements of the specimens. During the tests, the load versus vertical deformation was monitored continuously using an Hewlett Packard 7044A X-Y recorder. All data collected from the LVDT's and the load cell were recorded at approximately five second intervals by a data acquisition system. The axial deformation (δ) and failure load (P_{Test}) of each specimen are given in the columns (2) and (3) of Tables 5, 6, and 7.

To determine the material properties of the specimens, a series of tension tests were performed. Test coupons were cut from flat sheets as well as from randomly selected specimens which showed the least amount of damage due to testing. The tension tests were conducted in accordance with ASTM E 8M-85 Standard (1985). Table 8 lists the mechanical properties of the tensile coupons. The results given in this table indicate that there were two sets of steel sheets used in the investigation. For the first set, the average yield strength was 52.07 ksi (359 MPa) (standard deviation = 1.05) for the coupons cut from flat portions of test specimens (i.e., flanges, web, and edge stiffeners), while that for the second set was 47.03 ksi (324 MPa) (standard deviation = 0.69). According to ASTM A607-90a Standard (1991), the minimum requirement for tensile strength (F_u), yield strength (F_y), and percent elongation (ϵ) are 65 ksi (448 MPa), 50 ksi (345 MPa), and 20%, respectively. The results from the tensile coupons, shown in Table 8, are within the acceptable limits which is the 90% of the specified minimum values.

Observations made during the testing of all specimens indicated that the failure modes of these specimens depended on the width of the edge stiffeners. The predominant mode of failure, for specimens with no edge stiffeners or with narrow edge stiffeners, was distortional buckling of the flange-edge stiffener component followed by local buckling of the web. On the other hand, specimens with wider edge stiffeners, initially suffered localized buckling of the web followed by distortional buckling of the flange-edge stiffener component. A typical example of column specimens with edge stiffeners after failure is shown in Figure 4.

ANALYTICAL INVESTIGATION

The current North American design guidelines, AISI Specification (1989) and CSA Standard (1989), for cold-formed Z-sections were evaluated through comparison with the experimental results. The predicted results obtained from these design guidelines, along with the ratios between the experimental results and the predicted results, are given in Tables 5, 6, and 7.

The theoretical model used to simulate the behaviour of Z-sections is based on the assumption that the section will fail by distortional buckling of one or both flange-edge stiffener components. The distortional buckling stress of a flange-edge stiffener component is then taken as the critical stress of the whole section. If the distortional stress is less than the lateral or torsional stress, then it becomes the governing stress for which the load-carrying capacity of sections is computed without taking into account any post-buckling capacity. Otherwise, the failure is based on lateral or torsional behaviour of the member. The theoretical mode used for columns is illustrated in Figure 5. This model is based on the principle of column on elastic foundations, where the column consists of one of the flanges and its edge stiffener, while the elastic foundation is provided by the remaining portion of the member.

The governing differential equations for combined torsion and flexure for an undistorted section with continuous elastic supports were originally formulated by Vlasov (1961) and discussed in detail by Timoshenko and Gere (1961). Marsh (1985) and Lau and Hancock (1987) solved these simultaneous differential equations and proposed analytical procedures for obtaining the distortional buckling stress of thin-walled sections. These analytical procedures were further modified for the present theoretical model to reflect more realistically behaviour of cold-formed steel Z-sections.

In developing this theoretical model, it was assumed that a locally unstable web element can provide only vertical support to the flange-edge stiffener component. Thus, the elastic rotational and lateral restraints provided by the elastic foundation are assumed to be negligible and are thus not shown in Figure 5. All corners are assumed to be curved, as this is the case in cold-formed sections, and are included in the evaluation of the cross sectional properties of the flange-edge stiffener component. The modified expressions used to evaluate the distortional buckling load of the Z-section specimens is given in Appendix I. The predicted results obtained from the theoretical model, along with the ratios between the experimental and theoretical results, are given in Tables 5, 6, and 7.

COMPARISON OF ANALYTICAL RESULTS AND EXPERIMENTAL RESULTS

For each series of specimens, the ratios between experimental and predicted results are shown as functions of the overall width of edge stiffener in Figures 6 to 10. The experimental results along with the predicted results (AISI, CSA, and Theoretical curves) are also shown as functions of the overall width of edge stiffener in Figures 11 to 15. In these figures, the nominal cross sectional dimensions of the Z-section members and the specified minimum yield strength of 50 ksi (345 MPa) were employed in constructing the curves.

As shown in Figures 11 to 15, the values for the load-carrying capacity of the Z-sections with edge stiffeners computed according to the AISI Specification (1985) and the CSA Standard (1989) were always higher than the experimental results. Only those values corresponding to sections with no edge stiffeners were lower than the experimental results. The load-carrying capacity of this type of sections is limited to the local buckling capacity of the flanges in accordance with the design guidelines. The difference in treatment between sections with edge stiffeners and sections with no edge stiffeners resulted in the discontinuity shown in the AISI curves (Clauses C4(b) and C5) and the CSA curves (Clause C6.7.2) of Figures 11 to 15.

In order to evaluate the analytical results, the statistical values for the ratios between the experimental results and the analytical results obtained from each series of specimens are briefly discussed. For the 18 in. (457 mm) column specimens, according to the AISI Specification (1989) the ratio ranged from 1.37 to 3.31 for sections with no edge stiffeners, while the ratio ranged from 0.63 to 0.95 (average = 0.78; standard deviation = 0.083) for sections with edge stiffeners. According to the CSA Standard (1989), for the sections with no edge stiffeners the ratio ranged from 1.36 to 3.28, while for the sections with edge stiffeners the ratio ranged from 0.55 to 0.84 (average = 0.69; standard deviation = 0.069). According to the theoretical model, for all 18 in. (457 mm) column specimens the ratio ranged from 0.79 to 2.26 (average = 1.16; standard deviation = 0.280). In the case of the 24 and 48 in. (610 and 1219 mm) column specimens, according to the AISI Specification (1989) the ratios ranged from 2.75 to 3.24 and 2.96 to 3.28 for the sections with no edge stiffeners, while the ratios ranged from 0.80 to 1.11 and 0.81 to 1.11 (average = 0.92; standard deviation = 0.074, and average = 0.93; standard deviation = 0.074) for the sections with edge stiffeners. According to the CSA Standard (1989), for the sections with no edge stiffeners the ratios ranged from 2.72 to 3.21 and 2.93 to 3.25, while for the sections with edge stiffeners the ratios ranged from 0.76 to 1.05 and 0.77 to 1.06 (average = 0.84; standard deviation = 0.079, and average = 0.87; standard deviation = 0.075). According to the theoretical model, for all 24 and 48 in. (610 and 1219 mm) column specimens, the ratios ranged from 1.11 to 2.35 and 1.07 to 2.38 (average = 1.47; standard deviation = 0.338, and average = 1.39; standard deviation = 0.331).

CONCLUSIONS

This paper deals with the analytical and experimental investigation of cold-formed steel Z-sections loaded under direct compression. The results of 85 Z-sections of various cross sectional dimensions are presented and discussed. A simplified theoretical model is presented. This model was developed on the assumption that local buckling of the web followed by distortional buckling of the flange-edge stiffener components govern the mode of failure. Comparisons between the experimental results and the analytical results (AISI, 1989 and CSA, 1989) underestimated the load-carrying capacity of Z-sections with no edge stiffeners, whereas they overestimated the load-carrying capacity of those sections with edge stiffeners. By using the theoretical model, there is good correlation between the theoretical results and the experimental results. Also, the theoretical model provides a realistic representation of member behaviour for those sections with wider web and edge stiffeners where local buckling of the web precedes distortional buckling of the flange-edge stiffener component. As such, it may serve as a useful tool in evaluating the load-carrying capacity of cold-formed steel Z-section columns with slender webs.

ACKNOWLEDGEMENTS

The experimental investigation reported herein was sponsored by The Natural Sciences and Engineering Research Council of Canada (NSERC) and was carried out in the Civil Engineering laboratory of The University of Manitoba. The technical assistance provided by Mr. E. Lemke, Mr. M. McVey and Mr. G. Martin is gratefully acknowledged.

APPENDIX I. THEORETICAL MODEL

The load-carrying capacity of a Z-section was assumed to be that which corresponds to the distortional buckling capacity of the flange-edge stiffener component, as shown in Figure 5. Thus, the distortional buckling stress of the flange-edge stiffener component was multiplied by the gross cross sectional area of the whole Z-section to obtain the load-carrying capacity; i.e,

$$P_{Theory} = \sigma_d A \tag{1}$$

where,

$$\sigma_d = \sigma_{de} \qquad if \quad \sigma_{de} \leq \frac{F_y}{2} \tag{2}$$

and,

$$\sigma_d = F_y \left(1 - \frac{F_y}{4\sigma_{de}}\right) \qquad if \quad \sigma_{de} > \frac{F_y}{2} \tag{3}$$

where,

$$\sigma_{de} = E(\xi - \sqrt{\xi^2 - 4.2\psi}) \; / \; 5NA_d \tag{4}$$

$$\xi = I_{cx}\left(b_f + r\right) + 2\bar{y}I_{cxy} + 0.9\frac{J_c N}{V} + \frac{I_{cy}V}{b_f + r} \tag{5}$$

$$\psi = V\left(I_{cx}I_{cy} - I_{cxy}^2\right) + \frac{I_{cy}J_cN}{b_f+r} \tag{6}$$

$$N = V\left(\frac{I_{cx}w}{t^3}\right)^{0.5} \tag{7}$$

$$V = \overline{x}_c^{\,2} + \frac{I_{cx} + I_{cy}}{A_d} \tag{8}$$

where, b_f and w are the flat widths of the flange in the flange-edge stiffener component and the web element, respectively; r is the centerline bend radius of flange-edge stiffener junction; x_c and y_c are x- and y-coordinates of the flange-web junction with respect to the centroid; t is the base thickness of the section; A is the gross cross-sectional area of the Z-section; A_d is the full cross-sectional area of the flange-edge stiffener component; F_y is the yield strength of the steel; E is its modulus of elasticity; I_{cx}, I_{cy} and I_{cxy} are moments of inertia for effective section, and J_c is the torsional constant of the flange-edge stiffener component.

APPENDIX II. REFERENCES

American Iron and Steel Institute, (1989), "Specification for the Design of Cold-Formed Steel Structural Members," Part I of Cold-Formed Steel Design Manual, N.W., Washington, D.C., USA.

American Society for Testing and Materials, (1985), "ASTM E 8M-85 Standard Methods for Tension Testing of Metallic Materials," Philadelphia, USA.

American Society for Testing and Materials, (1991), "ASTM A607-90a Standard Specification for Steel, Sheet and Strip, High-Strength, Low-Alloy, Columbium or Vanadium, or Both, Hot-Rolled and Cold-Rolled," Philadelphia, USA.

Charnvarnichborikarn, P., and Polyzois, D. (1990), "Experimental and Analytical Investigation of Cold-Formed Z-Section Steel Members in Compression," Research Report, Department of Civil Engineering, The University of Manitoba, Winnipeg, Manitoba, Canada.

Cohen, J.M., and Pekoz, T. (1989), "Local Buckling Behavior of Plate Elements," Proceedings of the Sessions Related to Steel Structures at Structures Congress, ASCE, N.Y., USA., pp.235-244.

Desmond, T.P. (1978), "The Behaviour and Strength of Thin-Walled Compression Elements with Longitudinal stiffeners," Research Report No. 369, Department of Structural Engineering, Cornell University, Ithaca, N.Y., USA.

Lau, S.C.W., and Hancock, G.T., (1987), "Distortional Buckling Formulas for Channel Columns," Journal of Structural Engineering, ASCE, Vol.13, No.5, pp.1063-1078.

Le, Q.P., Polyzois, D., and Charnvarnichborikarn, P., (1990), "Behaviour of Cold-Formed Steel Members in Compression," Research Report, Department of Civil Engineering, The University of Manitoba, Winnipeg, Manitoba, Canada.

Marsh, C., (1985), "Influence of Lips on Flanges and Angles," Unpublished technical note of Canadian Standard Association, CSA, Canada.

Rosner, C.N., Polyzois, D., and Charnvarnichborikarn, P., (1989), "An Experimental Investigation on the Behaviour of Cold-Formed Steel Columns," Research Report, Department of Civil Engineering, The University of Manitoba, Winnipeg, Manitoba, Canada.

Timoshenko, S.P., and Gere, J.M., (1961), "Theory of Elastic Stability," McGraw-Hill Book Co. Inc., N.Y., USA.

Vlasov, V.Z., (1961), "Thin Walled Elastic Beams," 2nd., Israel Program for Scientific Translations, Jerusalem, Israel.

APPENDIX III. NOTATION

The following symbols are used in this paper:

A = gross cross sectional area of member;
A_d = cross sectional area of flange-edge stiffener component;
b, b_f = flat width of the flanges;
c = flat width of the straight edge stiffeners;
C_w = warping constant of flange-edge stiffener component;
D = overall width of edge stiffener;
E = elastic modulus of the cold-formed steel;
F_y = yield strength of the cold-formed steel;
F_u = tensile strength of the cold-formed steel;
I_{cx}, I_{cy} = moments of inertia of flange-edge stiffener component about the x- and y-axes, respectively;
I_{cxy} = product moment of inertia of flange-edge stiffener component about the x- and y-axes;
J_c = torsional constant of flange-edge stiffener component;
k_x, k_y, k_ϕ = stiffnesses of lateral and rotational restraints;
L = length of members;
P_{AISI} = predicted load-carrying capacity obtained through the AISI Specification (1989);
P_{Test} = load-carrying capacity obtained through testing;
P_{Theory} = proposed load-carrying capacity given by Equation 4;
P_{CSA} = predicted load-carrying capacity obtained through the CSA Standard (1989);
r = centerline bend radius of flange-edge stiffener junction;
t = base thickness of cold-formed section;
w = flat width of web element;
x_{co}, y_{co} = x- and y-coordinates of the shear centre (see Figure 5);
x_c, y_c = x and y coordinates of flange-web junction with respect to the centroid;
ϵ = percent elongation of the cold-formed steel;
δ = axial longitudinal deformation;
θ = angle between edge stiffener and flange element;

σ_{de}	=	elastic distortional stress of flange-edge stiffener component;
σ_d	=	inelastic distortional stress of flange-edge stiffener component.

TABLE 1 List of Test Variables and Number Specimens Tested
(Numbers in Brackets Indicate Numbers of Specimens Tested)

Specimen Type	L	θ	r	t	w	b_f	c (in.)									
	(in.)	(°)	(in.)	(in.)	(in.)	(in.)	-	0.00	0.15	0.25	0.50	0.75	1.00	1.25	1.50	2.00
(1)	(2)	(3)	(4)	(5)	(6)	(7)	(8)	(9)	(10)	(11)	(12)	(13)	(14)	(15)	(16)	(17)
Columns	18	90	0.28	0.059	4.0	1.50	[3]	-	-	[3]	[3]	[3]	[3]	-	-	-
	18	90	0.28	0.059	4.0	2.00	[3]	-	-	[3]	[3]	[3]	[3]	-	-	-
	18	90	0.28	0.059	4.0	2.50	[3]	-	-	[3]	[3]	[3]	[3]	-	-	-
	24	90	0.12	0.059	7.7	2.70	[2]	[2]	[2]	[2]	[2]	[2]	[2]	[2]	[2]	[2]
	48	90	0.12	0.059	7.7	2.70	[2]	[2]	[2]	[2]	[2]	[2]	[2]	[2]	[2]	[2]

Note : 1 in. = 25.4 mm

TABLE 2. Average Cross Sectional Dimensions of the 18 in. (457 mm) Specimens

Specimens (1)	L(in.) (2)	θ(°) (3)	w(in.) (4)	b_f(in.) (5)	c(in.) (6)	r(in.) (7)	t(in.) (8)	D(in.) (9)
1.50-0.00-1[a]	18.03	-	4.03	1.50	-	0.28	0.060	0.06
1.50-0.00-2[a]	18.03	-	3.99	1.51	-	0.28	0.059	0.06
1.50-0.00-3[a]	18.00	-	4.02	1.51	-	0.28	0.058	0.06
1.50-0.25-1	18.00	90.5	3.96	1.50	0.29	0.28	0.060	0.60
1.50-0.25-2	18.03	90.0	3.97	1.50	0.29	0.29	0.059	0.61
1.50-0.25-3	18.02	90.0	3.98	1.52	0.28	0.28	0.059	0.59
1.50-0.50-1	18.00	89.8	3.97	1.50	0.52	0.29	0.059	0.84
1.50-0.50-2	18.00	89.8	3.98	1.51	0.54	0.29	0.059	0.86
1.50-0.50-3	18.02	89.8	3.97	1.50	0.53	0.28	0.059	0.84
1.50-0.75-1	18.03	89.8	3.98	1.50	0.78	0.28	0.058	1.09
1.50-0.75-2	18.00	89.8	3.99	1.52	0.77	0.28	0.058	1.08
1.50-0.75-3	18.02	90.3	3.96	1.50	0.76	0.29	0.059	1.08
1.50-1.00-1	18.02	90.0	3.97	1.51	1.01	0.28	0.059	1.32
1.50-1.00-2	18.00	90.0	3.99	1.50	1.01	0.29	0.059	1.33
1.50-1.00-3	18.02	90.3	4.00	1.51	1.02	0.28	0.059	1.33
2.00-0.00-1[a]	18.00	-	4.04	2.00	-	0.29	0.059	0.06
2.00-0.00-2[a]	18.02	-	4.04	2.00	-	0.29	0.058	0.06
2.00-0.00-3[a]	18.02	-	4.07	2.00	-	0.27	0.058	0.06
2.00-0.25-1	18.02	89.0	4.01	2.00	0.30	0.28	0.058	0.61
2.00-0.25-2	18.02	89.5	3.96	1.99	0.28	0.29	0.059	0.60
2.00-0.25-3	18.02	89.0	3.98	1.99	0.30	0.28	0.059	0.61
2.00-0.50-1	18.00	90.3	3.95	2.01	0.53	0.28	0.059	0.84
2.00-0.50-2	18.00	89.8	3.97	2.00	0.54	0.28	0.059	0.85
2.00-0.50-3	18.00	90.3	3.93	2.00	0.52	0.28	0.059	0.83
2.00-0.75-1	18.02	90.3	3.99	1.98	0.78	0.29	0.058	1.10
2.00-0.75-2	18.02	90.0	3.99	1.98	0.79	0.29	0.058	1.10
2.00-0.75-3	18.02	89.8	3.99	1.99	0.77	0.29	0.058	1.09
2.00-1.00-1	18.02	90.0	4.00	2.00	1.00	0.28	0.058	1.31
2.00-1.00-2	18.03	89.8	3.98	2.00	1.02	0.28	0.057	1.33
2.00-1.00-3	18.02	89.8	3.97	2.00	1.01	0.29	0.059	1.33
2.50-0.00-1[a]	18.03	-	4.06	2.48	-	0.29	0.059	0.03
2.50-0.00-2[a]	18.03	-	4.07	2.48	-	0.29	0.059	0.03
2.50-0.00-3[a]	18.03	-	4.03	2.50	-	0.28	0.059	0.03
2.50-0.25-1	18.03	89.5	3.96	2.52	0.27	0.29	0.059	0.59
2.50-0.25-2	18.03	89.0	3.99	2.50	0.28	0.29	0.058	0.60
2.50-0.25-3	18.03	90.0	4.02	2.50	0.28	0.28	0.059	0.59
2.50-0.50-1	18.02	89.5	3.96	2.51	0.53	0.28	0.057	0.84
2.50-0.50-2	18.02	89.0	3.94	2.49	0.54	0.29	0.058	0.86
2.50-0.50-3	18.02	89.5	3.95	2.51	0.54	0.28	0.058	0.85
2.50-0.75-1	18.02	89.8	3.93	2.49	0.78	0.29	0.058	1.10
2.50-0.75-2	18.02	90.5	3.97	2.49	0.77	0.29	0.059	1.09
2.50-0.75-3	18.02	89.8	3.97	2.49	0.77	0.29	0.059	1.09
2.50-1.00-1	18.02	89.5	3.95	2.52	1.01	0.28	0.057	1.32
2.50-1.00-2	18.02	89.8	3.96	2.52	1.02	0.28	0.058	1.33
2.50-1.00-3	18.02	89.5	3.96	2.51	1.02	0.29	0.057	1.34

[a] Curved portion at the flange-edge stiffener junction not included

Note : 1 in. = 25.4 mm

TABLE 3. Average Cross Sectional Dimensions of the 24 in. (610 mm) Specimens

Specimen (1)	L(in.) (2)	θ(°) (3)	w(in.) (4)	b_f(in.) (5)	c(in.) (6)	r(in.) (7)	t(in.) (8)	D(in.) (9)
2.7-0.00-1[a]	23.99	-	7.70	2.83	-	0.16	0.058	0.06
2.7-0.00-2[a]	23.99	-	7.69	2.81	-	0.15	0.058	0.06
2.7-0.00-1[b]	24.02	90.0	7.72	2.75	0.00	0.14	0.058	0.17
2.7-0.00-2[b]	24.00	90.0	7.60	2.70	0.00	0.16	0.058	0.19
2.7-0.15-1	24.00	90.0	7.65	2.68	0.05	0.15	0.058	0.23
2.7-0.15-2	24.00	90.0	7.67	2.68	0.06	0.15	0.058	0.24
2.7-0.25-1	24.00	90.0	7.62	2.65	0.22	0.15	0.058	0.40
2.7-0.25-2	24.01	90.0	7.67	2.70	0.23	0.15	0.058	0.41
2.7-0.50-1	24.02	90.0	7.68	2.64	0.47	0.15	0.058	0.65
2.7-0.50-2	24.00	90.0	7.64	2.67	0.48	0.14	0.058	0.65
2.7-0.75-1	24.00	90.0	7.67	2.66	0.72	0.17	0.058	0.92
2.7-0.75-2	23.99	90.0	7.66	2.67	0.73	0.17	0.058	0.93
2.7-1.00-1	24.00	90.0	7.72	2.66	0.96	0.16	0.058	1.15
2.7-1.00-2	24.00	90.0	7.73	2.66	0.96	0.16	0.058	1.15
2.7-1.25-1	24.02	90.0	7.78	2.65	1.23	0.15	0.059	1.41
2.7-1.25-2	24.01	90.0	7.64	2.66	1.22	0.15	0.059	1.40
2.7-1.50-1	24.01	90.0	7.66	2.65	1.47	0.15	0.059	1.65
2.7-1.50-2	24.01	90.0	7.65	2.66	1.46	0.15	0.059	1.64
2.7-2.00-1	24.02	90.0	7.60	2.67	1.98	0.15	0.058	2.16
2.7-2.00-2	24.01	90.0	7.67	2.63	1.99	0.15	0.058	2.17

[a] Curved portion at the flange-edge stiffener junction not included
[b] Curved portion at the flange-edge stiffener junction included
Note : 1 in. = 25.4 mm

TABLE 4. Average Cross Sectional Dimensions of the 48 in. (1219 mm) Specimens

Specimen (1)	L(in.) (2)	θ(°) (3)	w(in.) (4)	b_f(in.) (5)	c(in.) (6)	r(in.) (7)	t(in.) (8)	D(in.) (9)
2.7-0.00-1[a]	48.03	-	7.75	2.81	-	0.16	0.058	0.06
2.7-0.00-2[a]	48.00	-	7.66	2.81	-	0.17	0.058	0.06
2.7-0.00-1[b]	48.03	90.0	7.56	2.57	0.08	0.16	0.058	0.27
2.7-0.00-2[b]	48.00	91.9	7.61	2.58	0.08	0.16	0.058	0.27
2.7-0.15-1	48.03	90.0	7.58	2.55	0.07	0.17	0.058	0.27
2.7-0.15-2	48.00	92.8	7.61	2.57	0.07	0.17	0.058	0.27
2.7-0.25-1	48.01	88.3	7.60	2.57	0.17	0.18	0.058	0.38
2.7-0.25-2	48.03	87.3	7.62	2.58	0.16	0.18	0.058	0.37
2.7-0.50-1	48.01	89.9	7.54	2.56	0.44	0.17	0.059	0.64
2.7-0.50-2	48.00	89.5	7.59	2.61	0.41	0.17	0.059	0.61
2.7-0.75-1	48.01	89.9	7.63	2.62	0.67	0.16	0.059	0.86
2.7-0.75-2	48.03	90.3	7.62	2.61	0.69	0.16	0.059	0.88
2.7-1.00-1	48.03	90.0	7.64	2.62	0.94	0.16	0.058	1.13
2.7-1.00-2	47.99	90.6	7.64	2.62	0.92	0.16	0.058	1.11
2.7-1.25-1	48.03	90.5	7.64	2.60	1.19	0.16	0.058	1.38
2.7-1.25-2	48.00	90.5	7.64	2.60	1.19	0.16	0.058	1.38
2.7-1.50-1	48.02	90.1	7.64	2.63	1.43	0.16	0.059	1.62
2.7-1.50-2	48.00	90.6	7.61	2.62	1.44	0.16	0.059	1.63
2.7-2.00-1	48.03	90.3	7.63	2.62	1.94	0.16	0.058	2.13
2.7-2.00-2	47.97	90.6	7.61	2.57	1.94	0.18	0.058	2.15

[a] Curved portion at the flange-edge stiffener junction not included
[b] Curved portion at the flange-edge stiffener junction included
Note : 1 in. = 25.4 mm

TABLE 5. Ratio Between Experimental Results and Analytical results for 18 in. (457 mm) Specimens

Specimens	TEST		AISI		CSA		THEORY	
	δ (in.)	P_{Test} (Kips)	P_{AISI} (Kips)	$\frac{P_{Test}}{P_{AISI}}$	P_{CSA} (kips)	$\frac{P_{Test}}{P_{CSA}}$	P_{Theory} (Kips)	$\frac{P_{Test}}{P_{Theory}}$
(1)	(2)	(3)	(4)	(5)	(6)	(7)	(8)	(9)
1.50-0.00-1[a]	0.08	11.90	8.60	1.38	8.69	1.37	11.90	1.00
1.50-0.00-2[a]	0.08	11.05	8.05	1.37	8.13	1.36	11.15	0.99
1.50-0.00-3[a]	0.10	11.90	7.86	1.55	7.75	1.54	10.63	1.12
1.50-0.25-1	0.12	18.90	21.03	0.90	24.53	0.77	18.65	1.01
1.50-0.25-2	0.10	17.45	20.63	0.85	23.90	0.73	18.25	0.96
1.50-0.25-3	0.13	19.30	10.30	0.95	23.51	0.82	18.01	1.07
1.50-0.50-1	0.09	17.90	24.10	0.74	26.86	0.67	19.28	0.93
1.50-0.50-2	0.13	19.90	24.21	0.82	26.92	0.74	19.33	1.03
1.50-0.50-3	0.13	15.25	23.96	0.64	29.72	0.57	19.23	0.79
1.50-0.75-1	0.13	18.10	23.24	0.78	25.80	0.70	18.83	0.96
1.50-0.75-2	0.11	19.80	23.38	0.85	26.00	0.76	18.88	1.05
1.50-0.75-3	0.13	20.87	24.07	0.87	26.90	0.78	19.45	1.07
1.50-1.00-1	0.14	20.90	22.83	0.92	24.80	0.84	18.82	1.11
1.50-1.00-2	0.12	19.30	22.86	0.84	24.78	0.78	18.79	1.03
1.50-1.00-3	0.13	18.25	22.76	0.80	24.70	0.74	18.78	0.97
2.00-0.00-1[a]	0.08	11.20	5.24	2.15	5.26	2.13	7.43	1.51
2.00-0.00-2[a]	0.08	11.85	4.95	2.40	4.99	2.37	7.06	1.68
2.00-0.00-3[a]	0.10	11.90	4.93	2.41	4.98	2.39	7.03	1.69
2.00-0.25-1	0.10	17.48	20.61	0.85	23.89	0.73	15.51	1.13
2.00-0.25-2	0.10	17.70	21.10	0.84	24.42	0.72	16.06	1.10
2.00-0.25-3	0.12	16.49	21.11	0.78	24.57	0.67	16.17	1.02
2.00-0.50-1	0.11	17.60	23.51	0.75	27.49	0.64	18.37	0.96
2.00-0.50-2	0.10	15.10	23.64	0.64	27.58	0.55	18.48	0.82
2.00-0.50-3	0.14	20.05	23.35	0.86	27.37	0.73	18.32	1.09
2.00-0.75-1	0.14	16.00	25.48	0.63	28.23	0.57	19.12	0.84
2.00-0.75-2	0.12	20.08	25.47	0.79	28.20	0.71	19.14	1.05
2.00-0.75-3	0.10	18.70	25.53	0.73	28.31	0.66	19.08	0.98
2.00-1.00-1	0.14	18.15	24.92	0.73	27.21	0.67	19.36	0.94
2.00-1.00-2	0.10	17.35	24.17	0.72	26.23	0.66	18.72	0.93
2.00-1.00-3	0.13	19.40	25.73	0.75	28.18	0.69	20.03	0.97
2.50-0.00-1[a]	0.09	12.05	3.76	3.21	3.79	3.18	5.50	2.19
2.50-0.00-2[a]	0.09	12.45	3.76	3.31	3.80	3.28	5.50	2.26
2.50-0.00-3[a]	0.10	12.20	3.69	3.31	3.72	3.28	5.41	2.25
2.50-0.25-1	0.10	15.80	21.45	0.74	24.48	0.65	13.18	1.20
2.50-0.25-2	0.11	17.60	21.02	0.84	23.98	0.73	12.91	1.36
2.50-0.25-3	0.14	19.80	21.39	0.93	24.48	0.81	13.25	1.49
2.50-0.50-1	0.10	16.40	23.03	0.71	26.61	0.62	15.23	1.08
2.50-0.50-2	0.13	19.10	23.86	0.80	27.64	0.69	16.10	1.19
2.50-0.50-3	0.12	18.65	23.72	0.79	27.50	0.68	15.92	1.17
2.50-0.75-1	0.13	18.60	26.93	0.69	29.65	0.63	18.13	1.03
2.50-0.75-2	0.13	20.00	27.70	0.72	30.67	0.65	18.70	1.07
2.50-0.75-3	0.14	19.10	27.70	0.69	30.67	0.62	18.70	1.02
2.50-1.00-1	0.13	19.00	25.78	0.74	27.94	0.68	18.47	1.03
2.50-1.00-2	0.12	18.89	26.51	0.71	28.84	0.65	19.19	0.98
2.50-1.00-3	0.15	18.00	25.80	0.70	28.03	0.64	18.58	0.97

[a] Curved portion at the flange-edge stiffener junction not included

Note : 1 Kip = 4.45 kN, 1 in. = 25.4 mm

TABLE 6. Ratio Between Experimental Results and Analytical results for 24 in. (610 mm) Specimens

Specimens	TEST		AISI		CSA		THEORY	
	δ (in.)	P_{Test} (Kips)	P_{AISI} (Kips)	$\frac{P_{Test}}{P_{AISI}}$	P_{CSA} (kips)	$\frac{P_{Test}}{P_{CSA}}$	P_{Theory} (Kips)	$\frac{P_{Test}}{P_{Theory}}$
(1)	(2)	(3)	(4)	(5)	(6)	(7)	(8)	(9)
2.70-0.00-1[a]	0.13	12.40	3.83	3.24	14.37	3.21	5.28	2.35
2.70-0.00-2[a]	0.12	10.60	3.86	2.75	14.20	2.72	5.32	1.99
2.70-0.00-1[b]	0.12	13.05	13.59	0.96	14.01	0.93	6.60	1.98
2.70-0.00-2[b]	0.13	11.15	13.91	0.80	14.33	0.78	6.93	1.61
2.70-0.15-1	0.14	12.80	14.75	0.87	15.55	0.82	7.45	1.72
2.70-0.15-2	0.13	12.35	14.93	0.83	15.80	0.78	7.59	1.63
2.70-0.25-1	0.15	15.20	17.09	0.89	19.13	0.79	9.95	1.53
2.70-0.25-2	0.14	15.80	17.23	0.92	19.32	0.82	9.90	1.60
2.70-0.50-1	0.16	18.90	19.85	0.95	23.14	0.82	13.40	1.41
2.70-0.50-2	0.14	18.25	19.82	0.92	23.12	0.79	13.27	1.38
2.70-0.75-1	0.15	20.56	23.92	0.86	26.65	0.77	16.06	1.28
2.70-0.75-2	0.16	20.40	24.11	0.85	26.72	0.76	16.10	1.27
2.70-1.00-1	0.16	20.70	23.84	0.87	26.04	0.79	17.65	1.17
2.70-1.00-2	0.17	20.85	23.84	0.87	26.04	0.80	17.66	1.18
2.70-1.25-1	0.15	23.10	23.95	0.96	25.97	0.89	19.26	1.20
2.70-1.25-2	0.16	21.25	23.99	0.89	26.03	0.82	19.21	1.11
2.70-1.50-1	0.17	23.40	23.39	1.00	25.12	0.93	19.32	1.21
2.70-1.50-2	0.17	21.90	23.45	0.93	25.19	0.87	19.33	1.13
2.70-2.00-1	0.18	23.30	21.06	1.11	22.14	1.05	17.38	1.34
2.70-2.00-2	0.17	20.90	20.85	1.00	21.89	0.95	17.23	1.21

[a] Curved portion at the flange-edge stiffener junction not included
[b] Curved portion at the flange-edge stiffener junction included
Note : 1 Kip = 4.45 kN, 1 in. = 25.4 mm

TABLE 7. Ratio Between Experimental Results and Analytical results for 48 in. (1219 mm) Specimens

Specimens	TEST		AISI		CSA		THEORY	
	δ (in.)	P_{Test} (Kips)	P_{AISI} (Kips)	P_{Test}/P_{AISI}	P_{CSA} (kips)	P_{Test}/P_{CSA}	P_{Theory} (Kips)	P_{Test}/P_{Theory}
(1)	(2)	(3)	(4)	(5)	(6)	(7)	(8)	(9)
2.70-0.00-1[a]	0.15	11.50	3.88	2.96	13.18	2.93	5.36	2.15
2.70-0.00-2[a]	0.17	12.70	3.87	3.28	13.35	3.25	5.34	2.38
2.70-0.00-1[b]	0.15	12.55	14.36	0.87	15.09	0.83	8.52	1.47
2.70-0.00-2[b]	0.18	11.65	14.38	0.81	15.10	0.77	8.49	1.37
2.70-0.15-1	0.16	12.90	14.35	0.90	15.01	0.86	8.61	1.50
2.70-0.15-2	0.15	12.70	14.21	0.89	14.86	0.85	8.40	1.51
2.70-0.25-1	0.14	13.70	15.77	0.87	17.10	0.80	9.99	1.37
2.70-0.25-2	0.15	14.30	15.66	0.91	16.92	0.85	9.80	1.46
2.70-0.50-1	0.18	19.40	19.34	1.00	22.26	0.87	14.36	1.35
2.70-0.50-2	0.18	16.90	18.90	0.89	21.71	0.78	13.63	1.24
2.70-0.75-1	0.21	20.95	22.12	0.95	24.48	0.86	16.33	1.28
2.70-0.75-2	0.17	20.80	22.61	0.92	25.58	0.81	16.63	1.25
2.70-1.00-1	0.17	21.45	22.46	0.95	24.44	0.88	17.68	1.21
2.70-1.00-2	0.18	19.60	22.48	0.87	24.48	0.80	17.57	1.12
2.70-1.25-1	0.20	20.55	22.16	0.93	23.82	0.86	18.60	1.11
2.70-1.25-2	0.21	22.30	22.31	1.00	23.97	0.93	18.60	1.20
2.70-1.50-1	0.20	20.75	22.50	0.92	24.04	0.86	19.35	1.07
2.70-1.50-2	0.22	21.45	22.59	0.95	24.11	0.89	19.33	1.11
2.70-2.00-1	0.21	21.75	20.31	1.07	21.22	1.02	17.38	1.25
2.70-2.00-2	0.22	22.55	20.32	1.11	21.19	1.06	17.20	1.31

[a] Curved portion at the flange-edge stiffener junction not included

[b] Curved portion at the flange-edge stiffener junction included

Note : 1 Kip = 4.45 kN, 1 in. = 25.4 mm

TABLE 8. Yield Strength of Tensile Coupons

Coupon Locations (1)	Coupon Specimens (2)	18 in. Z-Sections F_y (ksi) (3)	F_u (ksi) (4)	ϵ (%) (5)	24 and 48 in. Z-Sections F_y (ksi) (6)	F_u (ksi) (7)	ϵ (%) (8)
Virgin Sheet	1	51.01	73.02	28.40	47.95	71.07	29.28
	2	51.74	74.52	30.22	47.08	72.78	30.74
	3	52.53	74.96	22.55	47.71	72.08	29.88
	4	51.32	74.74	28.10	45.97	70.05	29.10
Flange	1	51.11	75.43	27.24	47.03	71.47	29.48
	2	52.27	75.56	27.56	47.56	70.66	30.74
	3	53.17	75.84	26.76	-	-	-
	4	50.54	75.31	27.22	-	-	-
Web	1	53.59	75.23	25.50	46.03	70.73	30.68
	2	52.82	74.77	27.24	47.64	71.55	28.22
Lip	1	51.61	74.97	26.48	47.56	70.40	29.28
	2	51.77	69.99	22.70	46.34	67.36	28.56
Corner	1	65.86	75.58	21.24	75.21	86.84	27.06
	2	67.69	76.78	21.32	76.48	88.04	30.92
	3	66.65	73.22	21.02	73.33	88.42	25.70

Note : 1 in. = 25.4 mm
1 ksi = 6.89 MPa

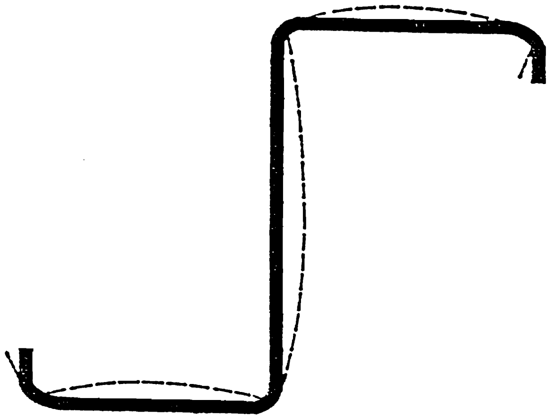

(a) Local Buckling

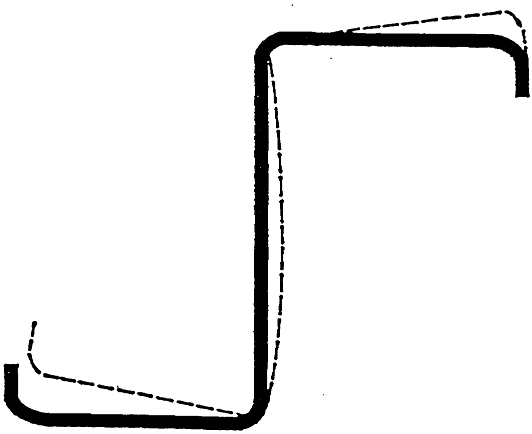

(b) Distortional Buckling

Figure 1 Buckling Behaviour of Cold-Formed Steel Z-Sections

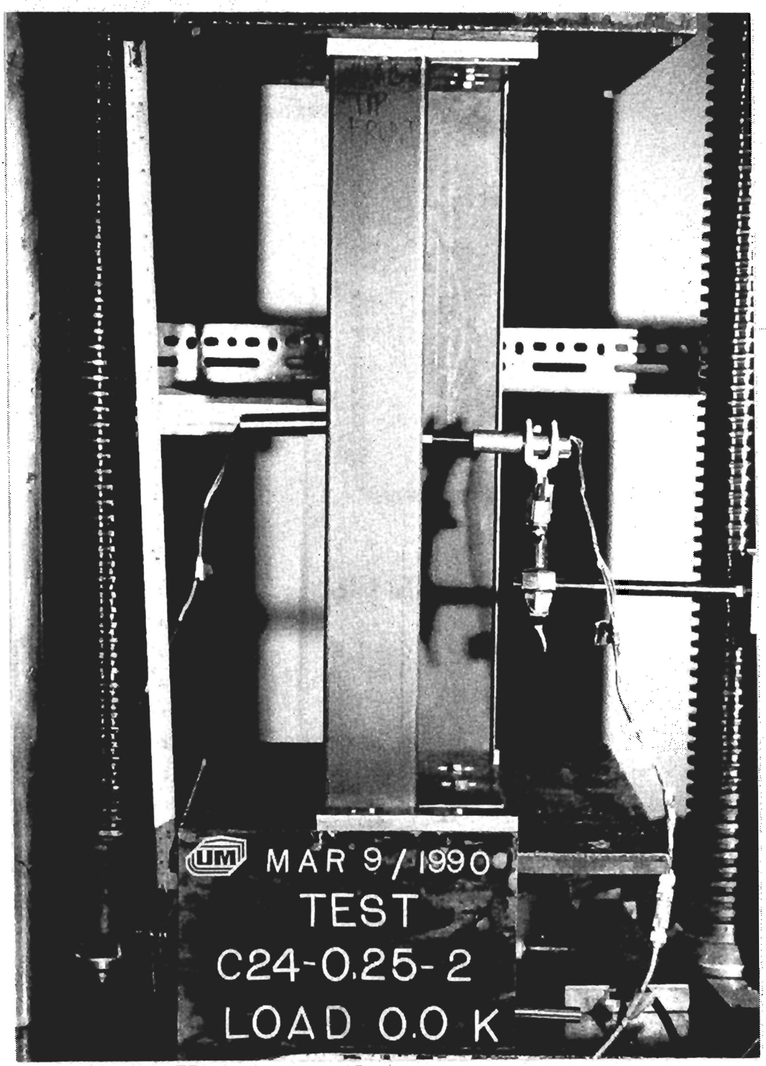

Figure 2 The Test Set-Up for a Typical Column Specimen

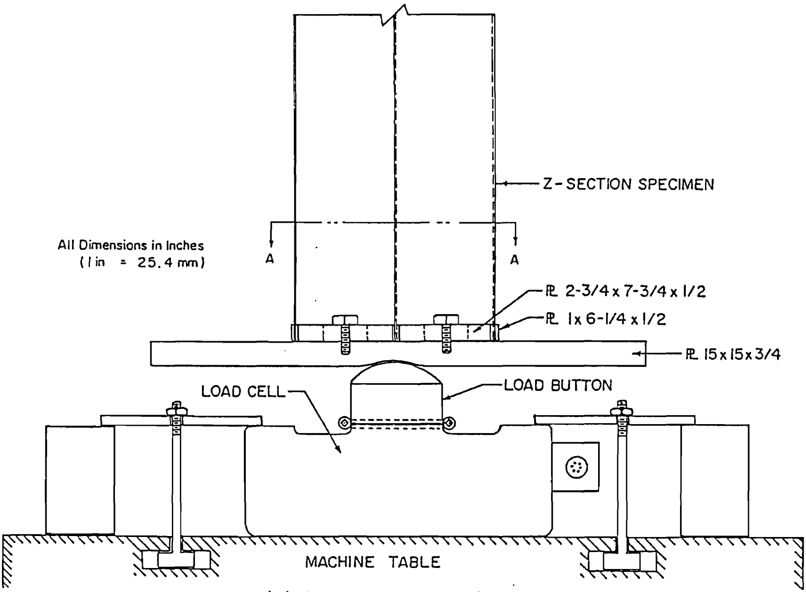

(a) Bottom Support Detail

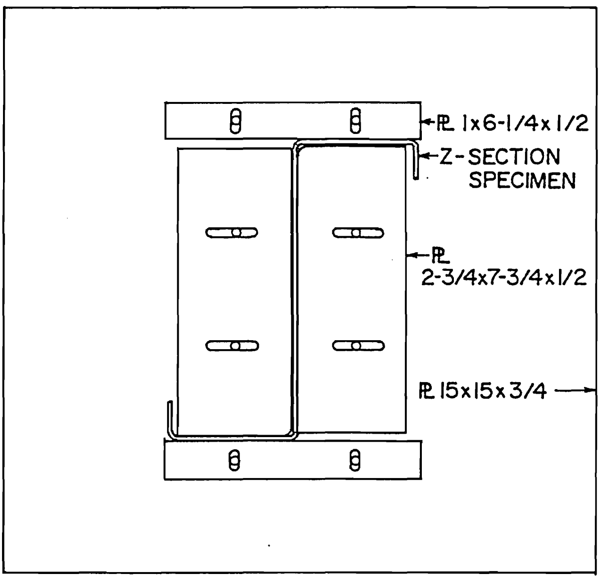

(b) Section A-A

Figure 3 Support Detail for Z-Section Specimens

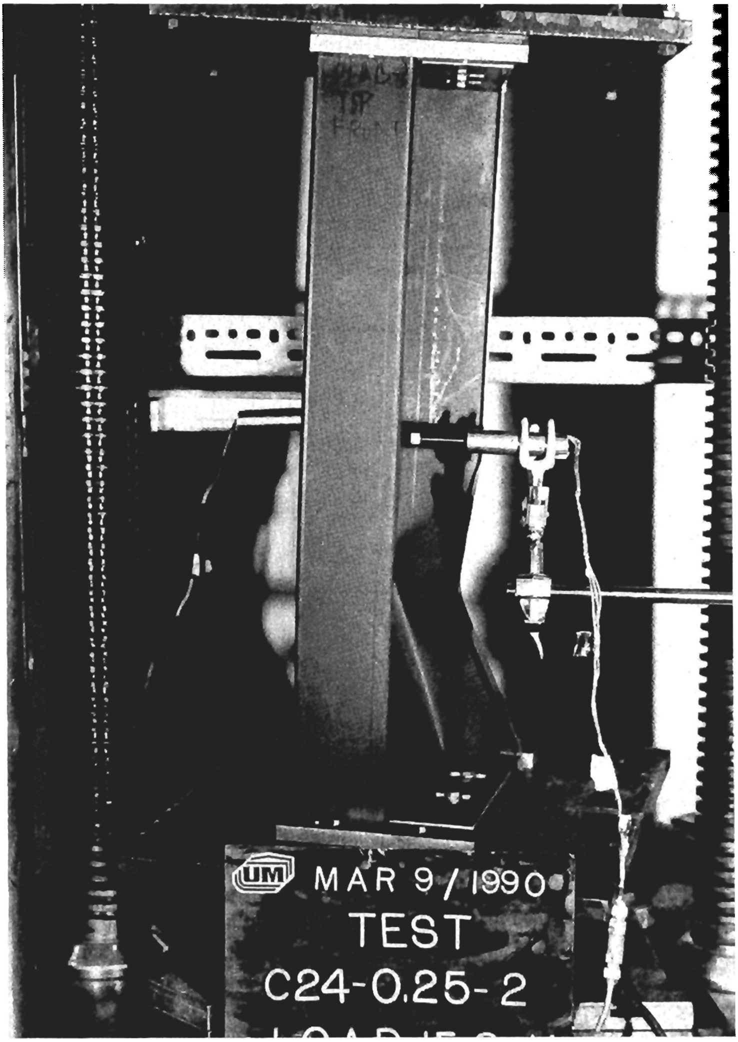

Figure 4 Z-Section Specimen after Failure

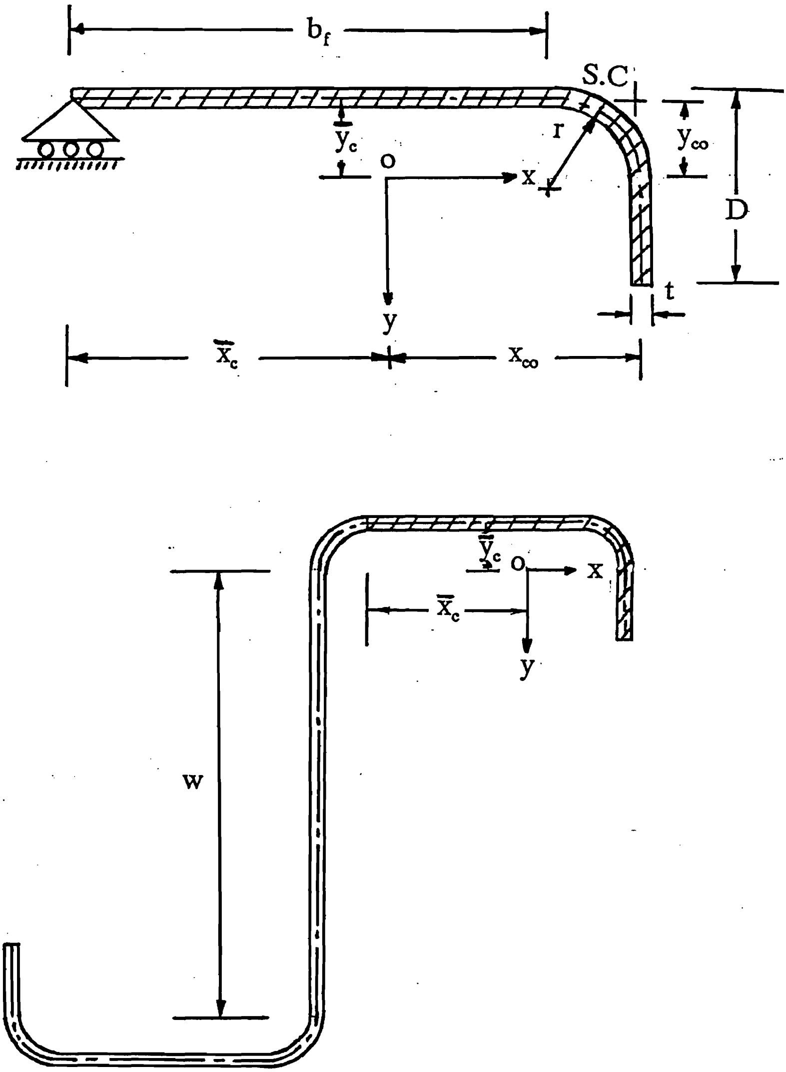

Figure 5 Theoretical Model of a Flange-Edge Stiffener Component for Cold-Formed Z-Section Columns

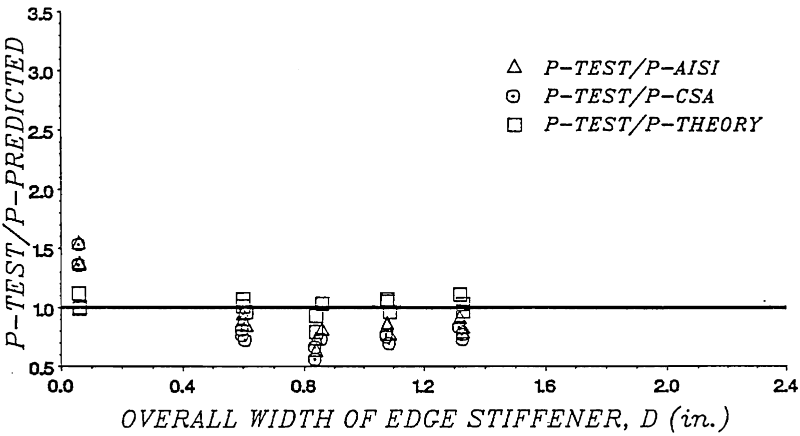

Figure 6 Analytical Load Ratios for 18 in. (457 mm) Specimens with 1.5 in. (38 mm) Flanges

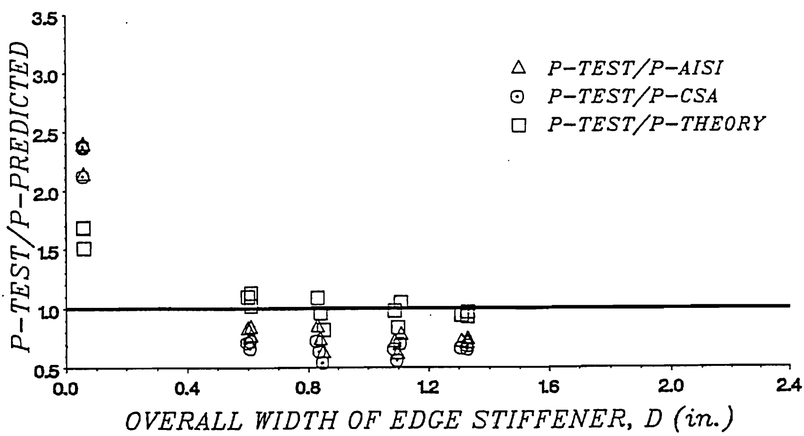

Figure 7 Analytical Load Ratios for 18 in. (457 mm) Specimens with 2.0 in. (51 mm) Flanges

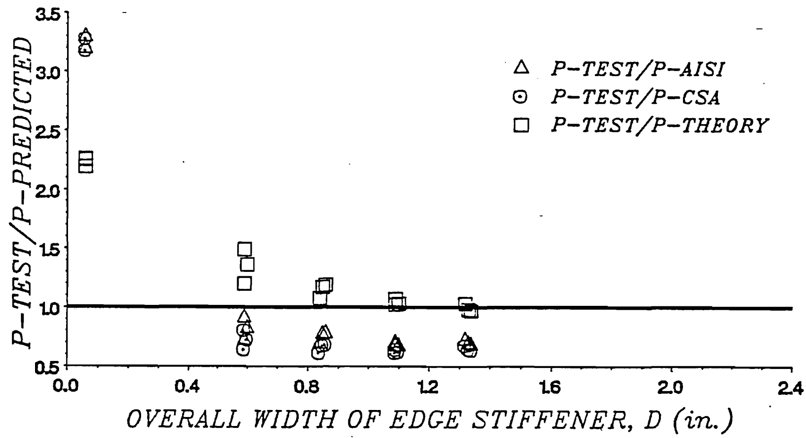

Figure 8 Analytical Load Ratios for 18 in. (457 mm) Specimens with 2.5 in. (64 mm) Flanges

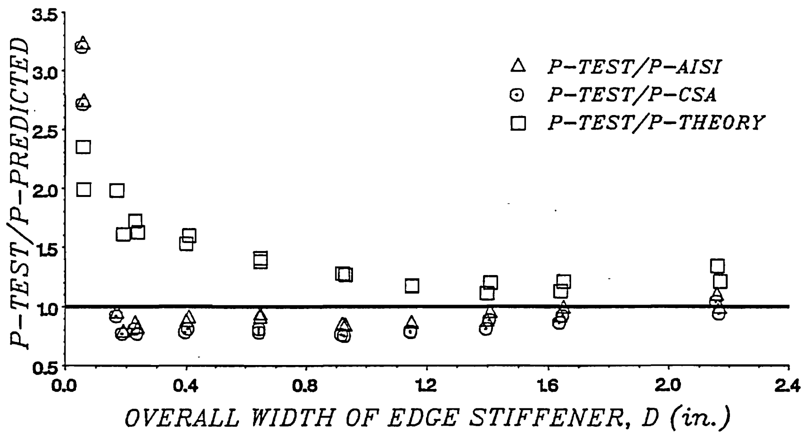

Figure 9 Analytical Load Ratios for 24 in. (610 mm) Specimens

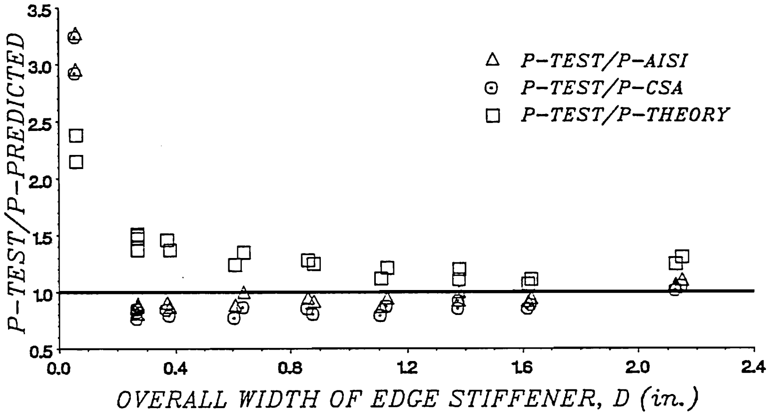

Figure 10 Analytical Load Ratios for 48 in. (1219 mm) Specimens

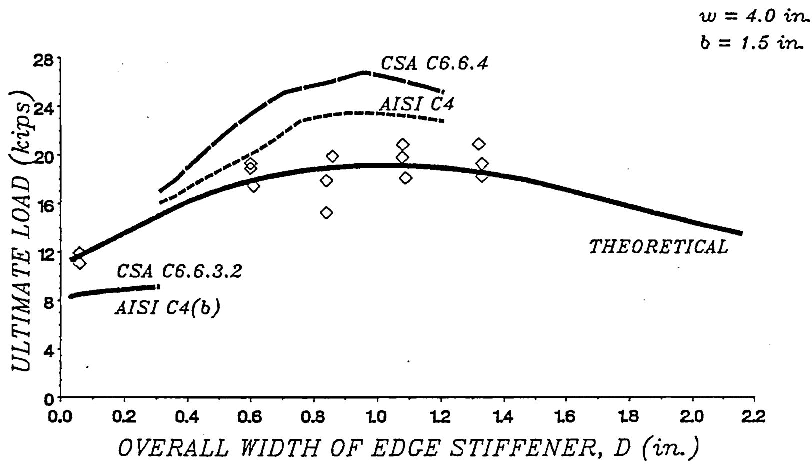

Figure 11 Experimental and Analytical Loads for 18 in. (457 mm) Specimens with 1.5 in. (38 mm) Flanges

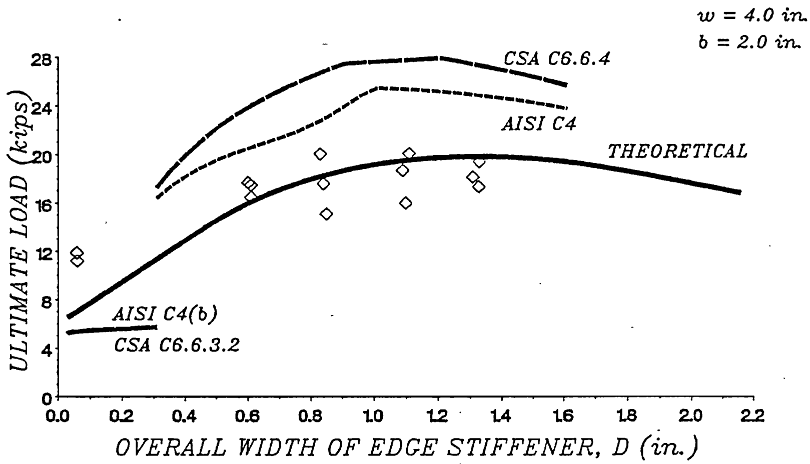

Figure 12 Experimental and Analytical Loads for 18 in. (457 mm) Specimens with 2.0 in. (51 mm) Flanges

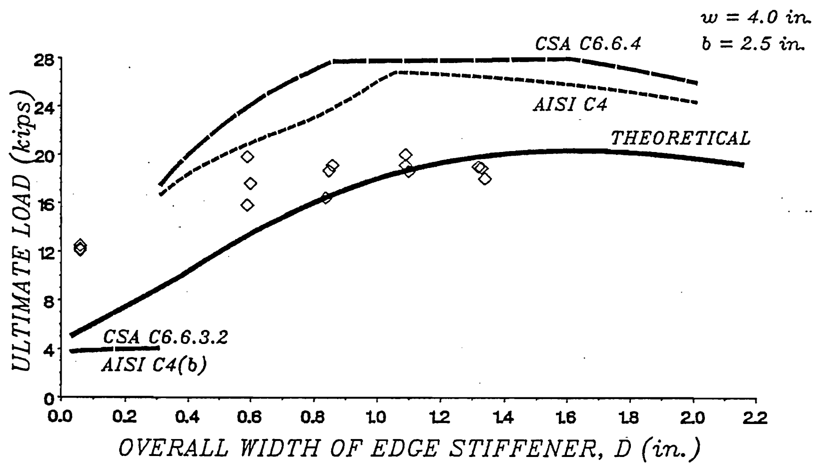

Figure 13 Experimental and Analytical Loads for 18 in. (457 mm) Specimens with 2.5 in. (64 mm) Flanges

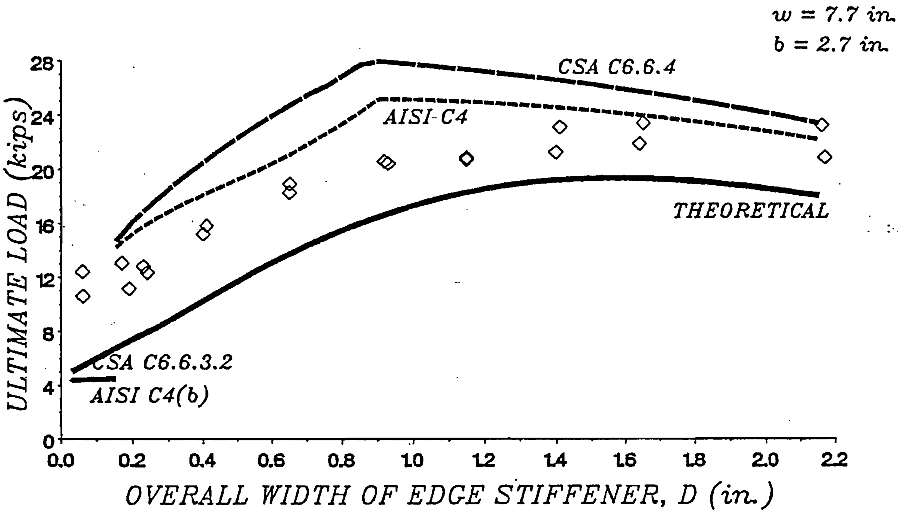

Figure 14 Experimental and Analytical Loads for 24 in. (610 mm) Specimens

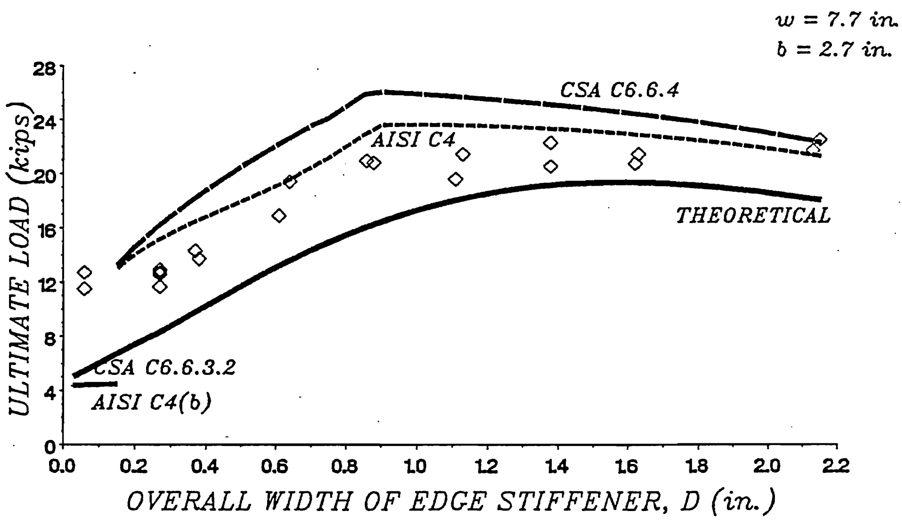

Figure 15 Experimental and Analytical Loads for 48 in. (1219 mm) Specimens